INSTITUTE OF PHYSICS PUBLISHING SEMICONDUCTOR SCIENCE AND TECHNOLOGY
Semicond. Sci. Technol. **16** (2001) 186–190 www.iop.org/Journals/ss PII: S0268-1242(01)18386-0

Optical and structural properties of self-organized InGaAsN/GaAs nanostructures

B V Volovik[1], A R Kovsh[1], W Passenberg[2], H Kuenzel[2], N Grote[2], N A Cherkashin[1], Yu G Musikhin[1], N N Ledentsov[1], D Bimberg[3] and V M Ustinov[1]

[1] Ioffe Physico-Technical Institute, 26 Polytekhnicheskaya Str., St Petersburg 194021, Russia
[2] Heinrich-Hertz-Institut für Nachrichtentechnik Berlin GmbH, Einsteinufer 37, D-10587 Berlin, Germany
[3] Technische Universität Berlin, Hardenbergstr. 36, 10623, Berlin, Germany

Received 28 October 2000, accepted for publication 15 January 2001

Abstract
Structural and optical properties of thin InGaAsN insertions in GaAs, grown by molecular beam epitaxy using an RF nitrogen plasma source, have been investigated. Nitrogen incorporation into InGaAs results in a remarkable broadening of the luminescence spectrum as compared with that of InGaAs layer with the same indium content. Correspondingly, a pronounced corrugation of the upper interface and the formation of well defined nanodomains are revealed in cross-sectional and plan-view transmission electron microscope (TEM) images, respectively. Raising the indium concentration in InGaAsN ($N < 1$ %) to 35 % results in the formation of well defined separated three-dimensional (3D) islands. The size of the nanodomains proves that the InGaAsN insertions in GaAs should be regarded as quantum dot structures even in the case of relatively small indium concentrations (25 %) and layer thicknesses (7 nm), which are below the values required for a 2D–3D transition to occur in InGaAs/GaAs growth. Dislocation loops have been found in TEM images of the structures emitting at 1.3 μm. They are expected to be responsible for the degradation of the luminescence intensity of such structures in agreement with the case of long-wavelength InGaAs-GaAs quantum dots.

1. Introduction

GaAs-based structures operating at 1.3 and 1.55 μm are much more attractive for injection lasers, compared with InP-based devices, owing to the higher temperature stability of the threshold current [1, 2] and the possibility of fabricating low-cost high-performance GaAs-based VCSELs [3, 4] making use of GaAs/AlGaAs Bragg mirrors. The most promising results have been obtained with InGaAs/GaAs [1, 3] and InGaAsN/GaAs structures [2, 4–7]. For the InGaAs/GaAs structures, the high lattice mismatch with the GaAs substrate stimulates the 2D–3D growth transition, leading to the formation of InGaAs quantum dots (QDs) emitting at wavelengths of up to 1.3 μm and beyond [8], owing to the relatively large volume of coherent InGaAs nanodomains. On the other hand, the long-wavelength luminescence from InGaAsN-based structures is mostly attributed to bandgap narrowing caused by nitrogen incorporation in the per cent range. The effects of surface corrugation have been either neglected because of the typically smaller indium content and partial lattice mismatch compensation by nitrogen atoms or expected to be only relevant to the case of a very high indium content [9]. However, the large (~ 20 %) difference between the radii of arsenic and nitrogen atoms may stimulate phase separation [10] and formation of nanodomains even in the case of a relatively small lattice mismatch with the substrate [11]. Moreover, the 2D–3D morphological transformation and phase separation may be interrelated, as observed in the case of activated decomposition of InGaAs alloy at InAs nanoscale stressors [12].

In this work, we investigated the optical and structural properties of InGaAsN insertions in GaAs, with varied content of In and N. We demonstrate that addition of N to InGaAs results in a significant broadening of the photoluminescence

 © 2001 IOP Publishing Ltd Printed in the UK

(PL) spectrum and attribute this phenomenon to the formation of narrow-gap nanodomains and the corresponding InGaAsN/GaAs interface corrugation. Clearly resolved isolated islands were revealed for the In content equal to 35 % (at N < 0.01). In addition, a high density of dislocation loops was revealed in TEM images of these structures. These dislocation loops are expected to be responsible for the degradation of the luminescence intensity, in agreement with the results obtained for long-wavelength InGaAs–GaAs QDs.

2. Experimental

The investigated structures were grown by molecular beam epitaxy (MBE) on GaAs semi-insulating substrates using solid sources of group III elements. A valved cracker source of arsenic was employed. Active nitrogen radicals were produced with an RF plasma source. The plasma source power was tuned in the range from 75 W to 150 W. The growth was carried out under As-rich conditions: the beam-equivalent pressure of As amounted to 1.5×10^{-5} Torr (which is 3 times the value necessary for the characteristic change of surface reconstruction from As-stabilized to group III-stabilized conditions). Two types of samples were grown: 0.2 μm thick GaAsN layers and thin (6–7 nm) InGaAsN single insertions, placed in the middle of a 0.2 μm thick GaAs layer confined by AlAs/GaAs short-period superlattices to prevent nonequilibrium carrier leakage to the surface and the substrate. The substrate temperature was maintained at 500 °C during growth of N-containing layers. The PL was excited by an Ar^+ laser ($\lambda \sim 514.5$ nm, $P \sim 100$ W cm^{-2}) and detected with a cooled Ge photodiode. Transmission electron microscopic (TEM) studies were carried out using a Philips EM 420 microscope operating at 100 kV.

3. Results and discussion

As a first step, we evaluated the efficiency of nitrogen incorporation into thick GaAsN layers. By comparing x-ray diffraction and PL data, we estimated the decrease in the GaAsN bandgap with increasing N content to be 160 meV per one per cent of N [13], in agreement with the data reported in [10]. Next, samples with thin (6–7 nm) InGaAsN insertions were studied. Figure 1(*a*) shows PL spectra of samples containing $In_{0.25}Ga_{0.75}AsN$ insertions with varied nitrogen content. Raising the N concentration (by increasing the input power of the nitrogen plasma source) leads to a red shift of the PL emission, broadening of the PL line, and a decrease in the integrated PL intensity. The last fact is typical of InGaAsN/GaAs samples [14, 15] and is usually attributed to an increase in the concentration of nonradiative recombination centres at higher nitrogen concentrations owing to the large difference in size between nitrogen and arsenic atoms [14] and/or to the surface damage by high energy ions coming from the RF plasma source [15].

We estimated the maximum N content in our samples to be as high as ~ 1.3 % at plasma source power of 150 W, assuming that the nitrogen incorporation efficiency is similar to that in GaAsN/GaAs growth. As it can be seen from figure 1, a significant increase in the PL full width at half-maximum (FWHM) from 45 meV up to 95 meV occurs with increasing

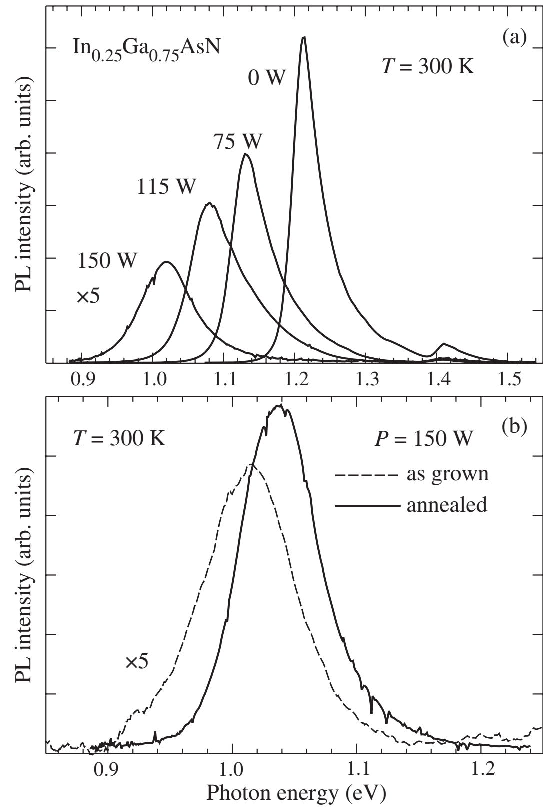

Figure 1. (*a*) PL spectra of samples with $In_{0.25}Ga_{0.75}AsN$ insertions in GaAs in relation to the N plasma source power (given as parameter near the spectra) and (*b*) the spectra before and after postgrowth anneal (700 °C, 30 minutes) for a sample grown with 150 W plasma source power applied.

N concentration. This effect has already been well documented for InGaAsN insertions [14], but the basic mechanism behind is still under discussion. The broadening may be related to either phase separation or interface corrugations on both nano- and microscale levels.

We checked the possibility of improving the PL intensity of InGaAsN insertions by using high temperature postgrowth annealing, as proposed by other authors [15, 16]. In our case, the annealing was performed at 700 °C for 30 min under a stabilizing As_4 flux (the annealing conditions were chosen so as to simulate the growth of an AlGaAs cladding layer in growing a laser structure). Figure 1(*b*) presents PL spectra of an $In_{0.25}Ga_{0.75}AsN$ sample (plasma source power 150 W) before and after annealing. The annealing led to a significant (7-fold) increase in the PL intensity, a relatively small PL blueshift of 20 meV and some moderate narrowing of the PL line. Previously, this effect has been attributed to In–Ga interdiffusion [11, 16]. In addition, samples with higher indium content $x_{In} = 0.3$ were investigated. The PL spectra of these samples are presented in figure 2. We note that the $In_{0.3}Ga_{0.7}As$ layer thickness of 7 nm, used in our case, was close to that at which the well known 2D–3D growth mode transformation occurs [17]. The parameters of this transition depend in part on some growth conditions, such as substrate temperature, arsenic pressure or surface misorientation. Under the growth conditions used in this work, the RHEED pattern was already spotty for the $In_{0.3}Ga_{0.7}As$ sample, indicating

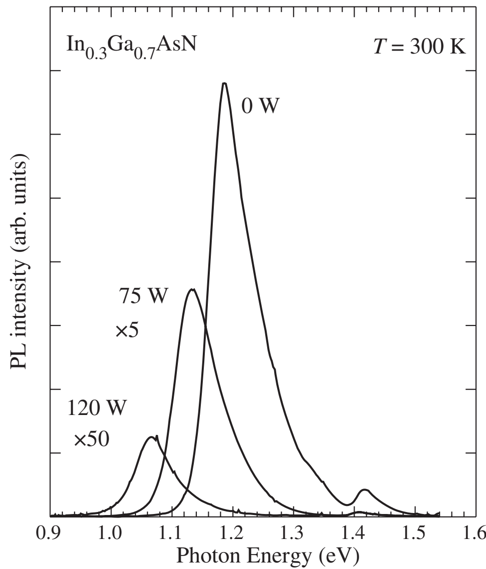

Figure 2. PL spectra of samples with $In_{0.3}Ga_{0.7}AsN$ insertions in GaAs in relation to the N plasma source power (given as parameter near the spectra).

a transition to the 3D growth. Addition of nitrogen must lead to partial compensation of the lattice mismatch with the substrate and, consequently, to stabilization of the 2D growth mode. However, we also observed a spotty RHEED pattern for $In_{0.3}Ga_{0.7}AsN$ samples. Moreover, for samples with a smaller indium content, where InGaAs/GaAs growth still showed a 2D behaviour, InGaAsN demonstrated a significant surface corrugation.

To investigate the amount of the corresponding surface corrugation and, additionally, the geometry and density of the domains formed, we carried out TEM studies both in plan-view and in cross-section geometries. Figure 3 presents plan-view and cross-section TEM images of InGaAsN/GaAs structures with varied In contents. It can be seen from the cross-section TEM images of the $In_{0.25}Ga_{0.75}AsN$ sample that the upper interface is significantly modulated, despite the relatively low In content and, therefore, the lower strain in this sample. The plan-view image of this sample shows ordered surface corrugation with characteristic size close to that observed in the cross-sectional images. A contrast typical of double-beam diffraction conditions (dark and bright parts separated by the zero contrast line) is observed in this image, originating from the domains and the deformation fields around them. The average domain size measured at the zero contrast line is approximately 45 nm, and the domain density is roughly 3×10^{10} cm^{-2}. We should note that $In_{0.25}Ga_{0.75}As$ insertions of the same thickness (7 nm) are well below the 2D–3D transition limit [17], as reflected by a narrow PL line (see figure 1). Furthermore, for $In_{0.25}Ga_{0.75}As$ insertions, a characteristic asymmetric band filling with increasing excitation density indicates a QW-like behaviour, in spite of the higher lattice mismatch with the GaAs substrate, compared with $In_{0.25}Ga_{0.75}AsN$. Thus, the observed thickness modulation is rather related to the nitrogen addition, despite the partial strain compensation. This finding indicates that, most probably, phase separation into the In-rich and In-poor regions occurs initially, giving rise to a weak bending of the surface. Further growth is influenced by activated alloy decomposition effects at the stressors formed, similarly to the case of activated decomposition of InGaAlAs at InAs QDs, resulting in increased domain volume and corrugation height [12].

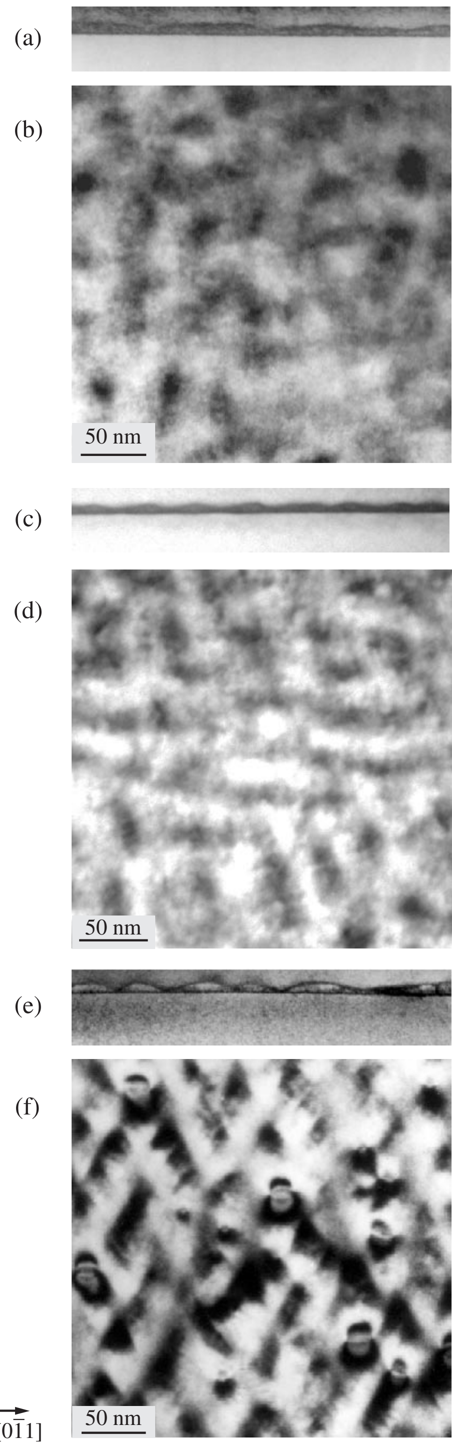

Figure 3. (*a*), (*c*), (*e*) Dark-field cross-section and (*b*), (*d*), (*f*) bright-field plan-view TEM images taken under double-beam conditions with $\boldsymbol{g} = (220)$ and $\boldsymbol{g} = (022)$, respectively, for samples with (*a*), (*b*) $In_{0.25}Ga_{0.75}AsN$ ($P_{plasma} \sim 115$ W); (*c*), (*d*) $In_{0.3}Ga_{0.7}AsN$ ($P_{plasma} \sim 115$ W) and (*e*), (*f*) $In_{0.35}Ga_{0.65}AsN$ ($P_{plasma} \sim 75$ W) insertions.

Following the trend depicted in figure 3, it can be concluded that raising the indium content of InGaAsN to 30 % leads to shrinkage of the average lateral size of the domain to approximately 35 nm, with the domain density increasing to about 4×10^{10} cm^{-2}. Further increase in the indium content to 35 % leads to the formation of well resolved quantum dots with average lateral size of 25 nm and height of 8 nm. The island density then increases to 5×10^{10} cm^{-2}. Furthermore, a high density of dislocation loops is seen in the plan-view images of this sample. We should note that a high concentration of defects has been revealed previously in samples with QDs formed by activated alloy decomposition with InGaAs overgrowth with high ($>$ 30 %) In content. Therefore, we attribute the relatively weak PL intensity of the sample with In content of 35 % to the defects observed, rather than to the high indium or nitrogen concentrations. The reasons for this conclusion are as follows: first, samples with comparable nitrogen concentrations demonstrate brighter PL at lower indium content, and, second, the sample with $In_{0.35}Ga_{0.65}As$ insertion exhibited 25 times higher PL intensity despite the stronger lattice mismatch. Thus, the decrease in the density of defects associated with the spontaneous formation of dislocated clusters seems to be of crucial importance for obtaining device quality material, as also found in the case of InGaAs/GaAs QD structures.

Long-wavelength emission near 1.3 μm at room temperature requires high In concentrations in InGaAsN (typically 30–35 % [5, 6]). Even without introduction of nitrogen, stimulating the formation of nanodomains (see above), such an In content may in itself result in a 2D–3D transition and nanodomain formation. Indeed, we observed a spotty RHEED pattern for 7 nm thick $In_{0.3}Ga_{0.7}As$ layer grown using our standard growth conditions.

To further investigate the domain formation in these structures, samples with $In_{0.3}Ga_{0.7}As$ insertions were grown at standard and enhanced (3 times higher) As fluxes. The use of higher As fluxes resulted in a dashed RHEED pattern for the same nominal layer parameters. Figure 4 shows PL spectra of $In_{0.3}Ga_{0.7}As$ insertions grown under standard and enhanced As fluxes, taken at different excitation densities. For the sample grown at a higher As flux only a single narrow peak is observed in the PL spectra at low excitation density. The increase in the excitation density results in band filling, the effect typical of quantum wells. For the standard As flux, we can clearly resolve two broad peaks in the PL spectra. The intensity of the low energy peak saturates with increasing excitation density. This behaviour is characteristic of QD structures with QD size dispersion and confirms the formation of 3D domains in this sample. In addition, cross-section TEM images of these two samples are shown as inserts in figure 4. It can be clearly seen that the enhanced As flux led to a uniform interface, while the standard As flux resulted in a strong surface corrugation. Thus, the 3D domain formation controlled by As flux variation can take place even without addition of nitrogen. On the other hand, addition of nitrogen further stimulates the island formation and even gives rise to domains in the samples with much smaller In concentration, despite the partial strain compensation. In addition, the PL emission from the sample with corrugated InGaAs/GaAs interface is shifted to longer wavelengths at smaller excitation densities. Therefore, the exact PL peak position is not only a function of the nominal In content but also depends on the growth mode involved.

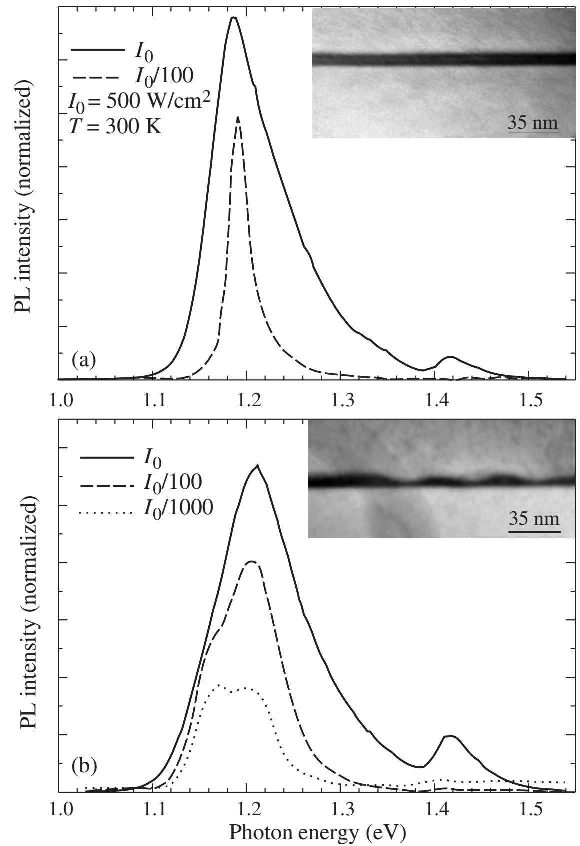

Figure 4. PL spectra and corresponding cross-section TEM images (shown as inserts) of samples with $In_{0.3}Ga_{0.7}As$ insertions in GaAs grown at (*a*) high and (*b*) standard As flux.

Long-wavelength emission near 1.3 μm at room temperature requires using relatively high concentrations of both In and N. Indeed, the transition energy for a 6 nm $In_{0.35}Ga_{0.65}As$ quantum well is only about 1.11 eV at room temperature [18]. We observed 1.32 μm emission for samples with 6 nm $In_{0.35}Ga_{0.65}As_{0.99}N_{0.01}$ insertions. Since our experimental data clearly indicate that such InGaAsN insertions indeed represent QDs, we can predict that some of the aspects of the InGaAsN/GaAs-based lasers may be similar to those appearing in QD lasers. Thus, such well known effects in QD lasers as the ground state gain saturation and the blue shift of the lasing wavelength with decreasing cavity length may also be relevant to the case of InGaAsN lasers. Furthermore, intentional use of the effects discussed here may be very useful for realization of InGaAsN QDs layers with low concentration of defects, emitting at longer wavelengths, which could be advantageous for 1.55 μm laser applications.

4. Conclusion

The optical and structural properties of thin GaAs-based InGaAsN insertions have been investigated. We attribute the PL properties of InGaAsN insertions to the nanodomains observed in TEM images. These nanodomains are even formed in the In content range exhibiting a 2D growth mode in the

absence of nitrogen. The lateral size of the nanodomains decreases with increasing In content. Raising the In content to above $x_{In} = 0.30$ in InGaAsN ($x_N < 0.01$) results in the formation of well defined separated 3D islands. We conclude that the InGaAsN insertions in GaAs should be regarded as QDs also in the case of relatively small indium concentrations ($x_{In} \sim 0.25$) and layer thicknesses (7 nm). Defects caused by locally formed dislocated clusters revealed in TEM images of structures emitting at 1.3 μm are believed to be responsible for the degradation of the luminescence intensity of long-wavelength InGaAsN insertions, similarly to the case of InGaAs/GaAs QDs.

Acknowledgment

This work was supported by the Russian Ministry of Science, Program 'Physics of Solid State Nanostructures', and NATO, 'Science for Peace' Program (project SFP-972484).

References

[1] Shernyakov Yu M *et al* 1999 *Electron. Lett.* **35** 898
[2] Sato S and Satoh S 1999 *IEEE Photonics Technol. Lett.* **11** 1560
[3] Lott J A *et al* 2000 *Electron. Lett.* **36** 1384
[4] Choquette K D *et al* 2000 *Electron. Lett.***36** 1388
[5] Egorov A Yu, Bernklau D, Livshits D, Ustinov V M and Alferov Zh I 1999 *Electron. Lett.* **35** 1643
[6] Kitatani T, Nakahara K, Kondow M, Uomi K and Tanaka T 2000 *Japan. J. Appl. Phys.* **39** L86
[7] Livshits D A, Egorov A Yu and Riechert H 2000 *Eletron. Lett.* **36** 1381
[8] Maximov M V *et al* 1999 *Appl. Phys. Lett.* **75** 2347
[9] Sopanen M, Xin H P and Tu C W 2000 *Appl. Phys. Lett. 76* 994
[10] Pozina G, Ivanov I, Monemar B, Thordson J V and Anderson T G 1998 *J. Appl. Phys.* **84** 3830
[11] Xin H P, Kavanagh K L, Zhu Z Q and Tu C W 1999 *Appl. Phys. Lett.* **74** 2337
[12] Volovik B V *et al* 1999 *Semiconductors* **33** 901
[13] Volovik B V, Kovsh A R, Passenberg W, Kuenzel H, Cherkashin N A, Musikhin Yu G, Ledentsov N N, Bimberg D, Ustinov V M 2000 *Proc. 8th Int. Symp. 'Nanostructures: Physics and Technology'* (St. Petersburg, Russia) p 148
[14] Xin H P and Tu C W 1998 *Appl. Phys. Lett.* **72** 2442
[15] Mars D E, Babic D I, Kneko Y, Chang Y L, Subramanya S, Kruger J, Perlin P and Weber E R 1999 *J. Vac. Sci. Technol.* B **17** 1272
[16] Kageyama T, Miyamoto T, Makino Sh, Koyama F and Iga K 1999 *Japan. J. Appl. Phys.* **38** L298
[17] Petroff P M and DenBaars S P 1994 *Superlattices Microstruct.* **15** 15
[18] Krijn M P C M 1991 *Semicond. Sci. Technol.* **6** 27